Effect of laser processing on the microstructure of the FeCrAl alloys

V. GEANTĂ[a], I. VOICULESCU[b,*], D. TENCIU[c], L. BASCHIR[c], E. M. STANCIU[d], A. PASCU[d]
[a]*Politehnica University of Bucharest, Obtaining Engineering and Management of Metallic Materials Department, 313, Splaiul Independentei, 060042, Bucharest, Romania*
[b]*Politehnica University of Bucharest, Quality Engineering and Industrial Technologies Department, 313, Splaiul Independentei, 060042, Bucharest, Romania*
[c]*National Institute of Research and Development in Optoelectronics INOE 2000, Romania*
[d]*Transilvania University of Braşov, 29 Eroilor Blvd., 500036, Braşov, Romania*

FeCrAl alloys are currently investigated in order to determine their behaviour at high temperatures in different environments, both erosive and corrosive (solid, liquid or gaseous). Nowadays, FeCrAl are used in special applications such as engine parts or various components of generation IV nuclear power plant were liquid metallic media is used for cooling. These media (like Pb, Pb-Bi, Sn) provide an increased heat transfer capacity. To increase the alloys resistance in extreme conditions (corrosion, erosion, high temperature) some surface processing can be performed to obtain a protective layer which constitute an effective barrier against the destructive action of the working environment. This study presents the results obtained by laser surface processing of several experimental FeCrAl alloys. Metallographic aspects such as microstructure changes, layer thickness and grain refining have been analysed. The microhardness values obtained in the processed layers are analysed, in comparison with the base metal and the results show that laser processing can be beneficial in terms of hardness increasing and grain refinement of FeCrAl alloys.

(Received July 31, 2020; accepted August 18, 2020)

Keywords: laser processing, microstructure, FeCrAl alloys, microhardness

1. Introduction

In fourth-generation nuclear power plants, the cooling is provided by metallic liquid media, such as Pb, Sn or PbBi. These environments allow a better functional parameter of the reactor by increasing the cooling efficiency. FeCrAl alloys have a higher content of Al and very low carbon content comparatively with the conventional ferritic stainless steels trademarks. The presence of Al and Cr in their chemical composition allows the formation of a thin and compact oxide layer, that can be grow using special thermal processing techniques like laser remelting. Usually, the FeCrAl alloys have a typical chemical composition of Fe + 20Cr + 5Al (wt.%) and are characterized by excellent mechanical and corrosion resistance at high temperatures (usually 800-1000 °C in industrial environment or 1200-1400 °C in the atmosphere), due to the alumina layer which has a low volatility above 1000 °C and protects the metal surface against degradation [1].

These alloys are currently used for the fabrication of engines components or as resistive elements of electric furnaces. The lower density (7.2 - 7.4 g/cm3) compared to low-aluminium content stainless steels (7.8 g/cm3) allow decreasing of fuel consumption and reducing the pollution effects [2], due to the high content of Al (4 - 20 wt.%). In order to achieve a good protective effect at the surface of the alloy, a minimum content of min. 2% Al is required [3].

For maintenance of the integrity of the protective layer at alloy surface, the FeCrAl can be supplementary alloyed with some reactive elements, such as Y, Hf, Zr, Ti, Ce, La, which reduce the oxidation and exfoliation effect of the oxide from the metal surface [3, 4].

The chemical elements like Y, Ce, La and Ti can form more stable sulphides than Al_2S_3, thus improving the adhesion of the protective layer and preventing the segregation of sulphur at the oxide / metal interface [5, 6 and 7]. The main problem that arises by using a metallic-ceramic layer is to ensure compactness and stability in the working conditions. In the case of alumina, there are a variety of polymorphic shapes (pyramid, columns, and whiskers) and configurations depending to the temperature and nature of the working medium (especially oxygen levels), that influence the surface roughness [8, 9]. It is well known that FeCrAl alloys are sensitive to grains coarsening during long exposures at high temperatures (800 – 1200 °C). By alloying with Mo and Nb, a favourable effect of reducing the grain dimensions and decreasing the probability of fragile phase's formation (Laves, M23C6 or M7C3) is obtained [10]. Special requirements and qualification of the alloys must be achieved, before using a new type of material in nuclear power plants [11]. The specific operating conditions of the 4R generation nuclear power plants refer to a new efficient cooling media (Lead and Bismuth) that allow the reduction of the reactor dimensions and also ensure a higher safety level. Considering that, strict control of the oxygen content in the cooling medium is essential. The oxygen content of

$1x10^{-6}$ wt% and $1x10^{-8}$ wt% O will produce a too thin or too thick layer of oxide, which may crack or peel-off under the action of the cooling liquid media [12-14]. Surface processing techniques applied to date have included the deposition of alumina-rich layers (for FeCrAlY alloys), followed by electron beam processing [13] or plasma processing [15].

It has been found that, in the case of FeCrAl alloy, a thin and compact layer of chromium oxide is first formed and then incorporated into the thicker layer of alumina [16]. In the case of flat surfaces, laser remelting can be an easy solution to ensure a low roughness, without imperfections, with a finer grain [17] and better corrosion resistance [18]. At the same time, the homogeneity of the layers deposited with plasma can be improved, by laser remelting [19] or selective laser polishing of thin surfaces (less than 5μ) [20]. It was found that by laser remelting of metallic-ceramic nanocomposite layers, an improved mechanical behaviour can be obtained [21-22].

The high energy density of the laser allows the processing of metallic or non-metallic materials with high precision and repeatability without direct contact with the material [23]. By laser irradiation a series of surface processing can be performed, such as: melting a thin layer of material, heat treatment, laser ablation or deposition of a metallic-ceramic layer by adding powders in the laser beam [23-26]. Effects of the laser irradiation combined with the increasing of chromium content, can modify the surface texture and roughness, and promote grain refinement followed by increase of microhardness [27-30].

This study aims to highlight the effects of surface laser processing on the microstructural characteristics of some experimental alloys of FeCrAl system. These special designed alloys contain different concentrations of Cr and Al, in order to determine their effects on the microstructure and microhardness proprieties. Obtaining of a thin metallic-ceramic layer with high corrosion resistance in molten metals is essential to ensure a good operating performance of the alloys in nuclear power plants. It was aimed, by laser surface processing, to refine the microstructure grains in order to obtain a better compactness necessary to increase the resistance to dissolution in the working environment. The experimental tests highlighted the microstructure changes, the compositional homogenization and the hardness increasing in the laser remelted areas.

2. Experimental

2.1. Materials

The special designed FeCrAl alloys were obtained in the Eramet laboratory from UPB Romania (Politehnica University of Bucharest), by melting in VAR (vacuum arc remelting in argon protective atmosphere) installation [27-29]. The samples were fabricated from high purity raw materials: very soft steel (MK3 brand) having the chemical composition of: C = 0.02%; Si = 0.04%; Mn = 0.21%; S = 0.02%; P = 0.015%; Ni = 0.2%; Cr = 0.15%; Mo = 0.07%; Cu = 0.14%; Al = 0.12% and Fe = balance %; metallic chromium with a minimum purity of 99% Cr; electrolytic aluminium, with a minimum purity of 99.5% Al.

To improve the homogeneity of the alloy, each sample was rotated and melted three times on each side. The chemical composition of the FeCrAl alloys samples were noted S1 to S4 and analysed with Spark Optical Emission Spectrometer – SPECTROMAXx M, as presented in table 1.

Table 1. Chemical composition of FeCrAl alloys

Sample	***Chemical composition, wt.%***			
	Cr	***Al***	***Fe***	***Other elements***
S 1	*8.3*	*6.2*	*80.9*	*4.5*
S 2	*10.7*	*5.1*	*83.1*	*1.1*
S 3	*13.9*	*4.1*	*81.1*	*0.9*
S 4	*16.2*	*4.1*	*78.8*	*0.9*

2.2. Laser surface processing

The heating source used for the surface processing/remelting of the FeCrAl samples was a 1kW continuous wave diode laser made by Coherent. The generated laser beam is in the near infrared region and has 975 nm wavelength and 56 mm*mrad maximum divergence. A six axes CLOOS robot was employed for the manipulation of the laser processing head (YW50 Precitec). A minimum tilt angle of 4˚ of the processing head was used to protect the laser optical system. The protection of melted bath was ensured by Argon gas coaxially provided within the laser beam at a flow rate of 6 l/min. The negative defocusing as illustrated in figure 1 was realized by changing the distance between the processing head and the material top surface.

A constant stand-off distance of 6mm was used for all the experimental tests. The main parameters of the laser processing regime are presented in Table 2.

The effect of laser irradiation on the proprieties of the remelted area was investigated by using 2 different processing parameters (regimes) on each sample.

Fig. 2 shows the FeCrAl samples after the laser surface processing.

Table 2. Laser processing parameters

Parameters / Regime	Power [W]	Processing speed [cm/min]	Spot diameter [mm]	Gas flow (Ar) [l/min]	Stand-off distance [mm]
1	320	80	1.1	7	6
2	500	80	1.1	6	6

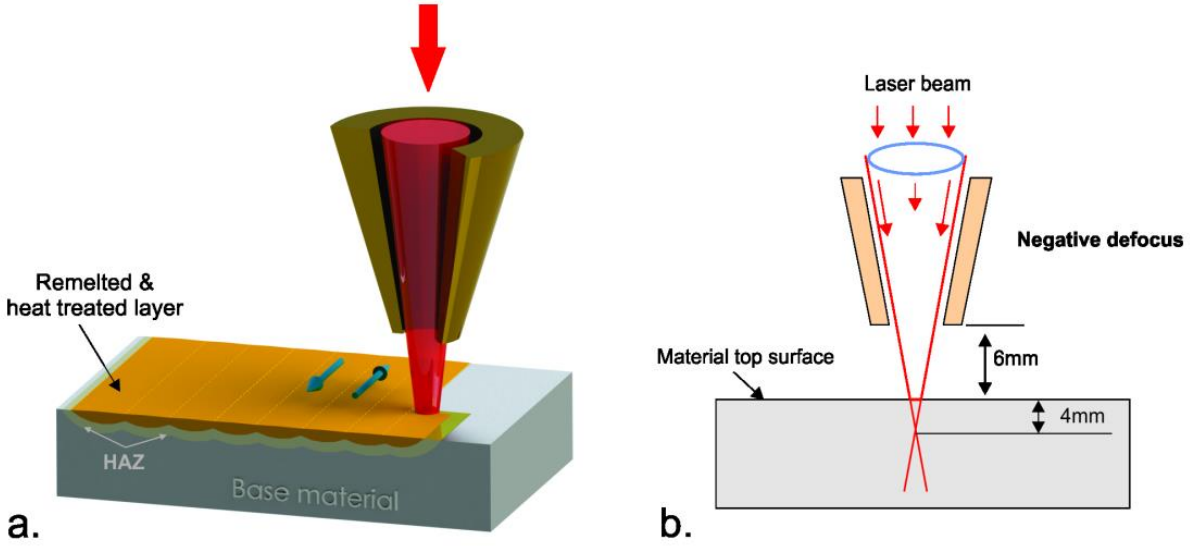

Fig. 1. Schematic of the laser processing/remelting process: a) laser system movement for surface remelting; (b) positioning the laser head and focus point in relation to the metal surface [30] (color online)

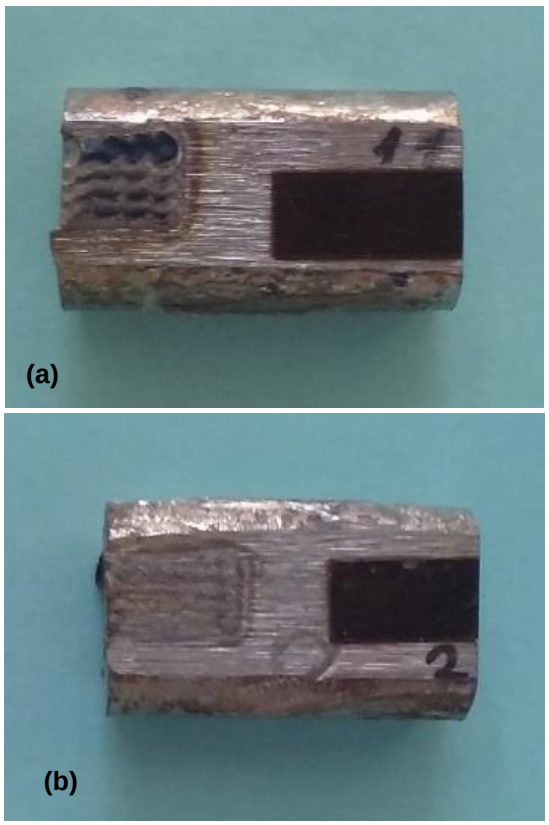

Fig. 2. Surface of the processed samples with laser; a) regime 1; b) regime 2 (color online)

3. Results and discussion

3.1. Microstructure

For the microstructural analysis, the specimens were prepared by cutting using high-precision discs (IsoMet 4000 cutting machine). The specimens were then embedded in phenolic resin and sanded with metallographic paper (grit paper of 360 to 1200) and then polished with alpha alumina powder (Topol1-3, powder diameter of 3 to 0,1 microns). To highlight the appearance of the remelted areas and to measure the penetration depth, an electrochemical etching in 10% oxalic acid solution-distilled water was applied (current 10A, time 15 sec). The metallographic analysis was performed with an Olympus GX51 optical microscope equipped with Analysis image processing software. In depth investigations was performed using an SEM Inspect S electron microscope, FEI, equipped with Z2e EDAX analyser.

The analysis of the test samples showed the as-cast microstructure, with coarse polyhedral grains of high alloyed ferrite. In areas remelted with laser, the microstructure contains fine dendrites oriented in the direction of heat flow, maintains the old grain boundaries of the base material (Fig. 3, optical microscopy - OM).

In order to compare the obtained results, the measurement of the laser melting depth was performed using the same magnification (200x). In the analysed samples, the chromium concentration has been increase

from 8.3 wt.% to 16.2 wt.% Cr, while the aluminium concentration has been decrease from 6.2 wt.% to 4.1 wt.% Al.

By laser surface processing of samples S1 to S4, different thicknesses of melted layers were obtained, depending on the laser power and the chemical composition of the alloy. Thus, in the case of the laser processing using a power of 320W, melting depths between 68µm (sample 3) and maximum 163µm (sample 1) were obtained. By increasing the laser power up to 500W, the melting depth increased from 393 µm (sample 3) to 519 µm (sample 1). The melting depth is mainly influenced by the quantity of Cr, a refractory element that reduces the heat transfer coefficient of the alloy [31-33]. At the same time, chromium contributes to the increase of hardness as being dissolved in Fe (highly alloyed ferrite) and by the formation of complex carbides [34]. Laser remelted layers have a fine, dendritic microstructure. The profile of the laser processed surface is more uneven in the case of the processing with the power of 320W, becoming smoother in the case of using 500W.

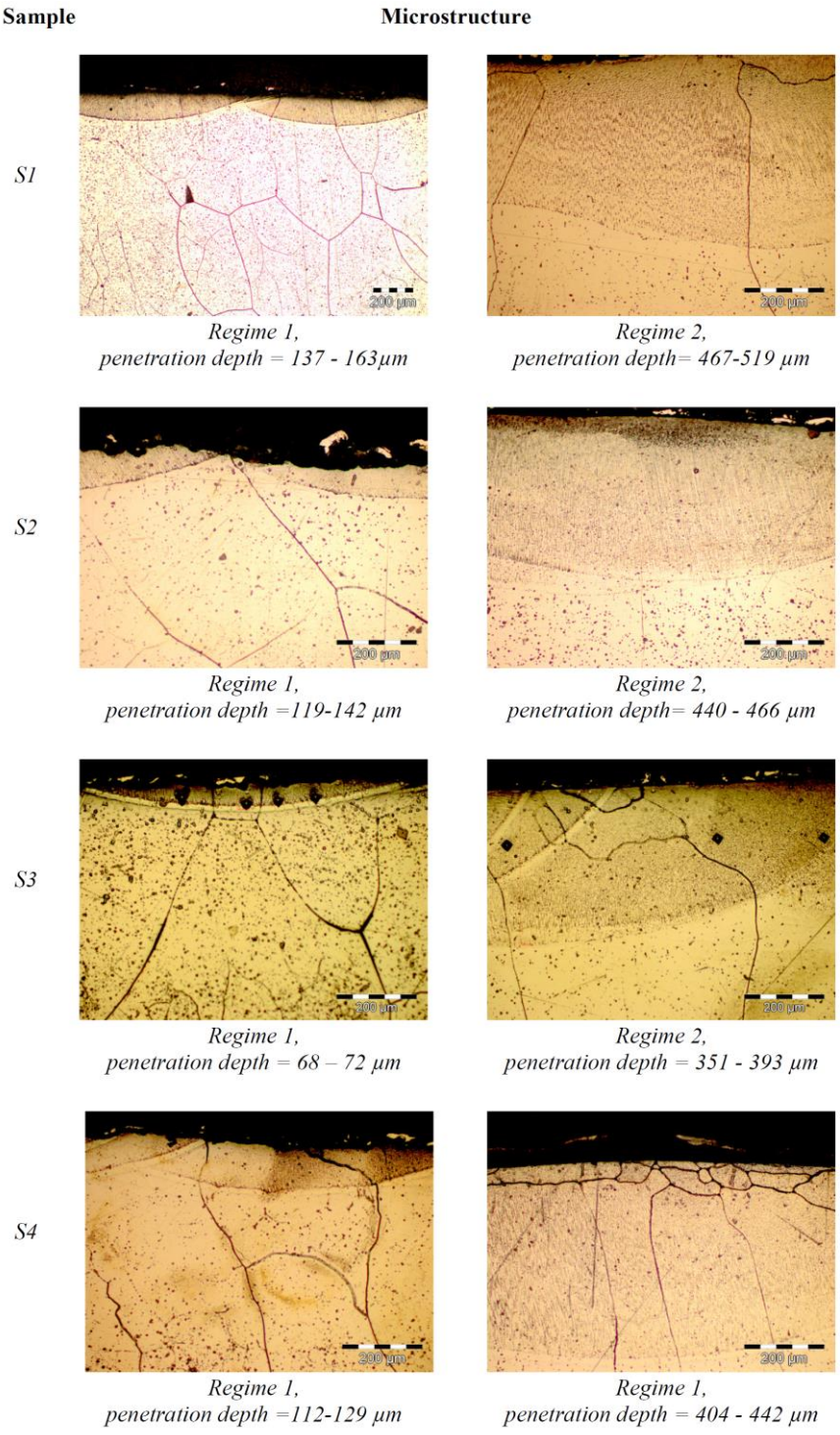

Fig. 3. Cross section of laser processed zones for FeCrAl experimental alloys (OM) (color online)

The effect of laser processing on the FeCrAl alloys was evaluated by SEM microscopy and EDAX analysis, determining the chemical compositions of the laser remelted areas and the adjacent ones.

In the case of Sample 1 (Fig. 4), there is a slight increase in the concentration of Cr (9.7 to 9.92 wt.%) and Al (6.54 to 6.93 wt.%).

In the laser remelted areas, a two-time grains refinement has been observed (from grains with an average diameter of 400 μm to about 200 μm). The increase of the oxygen concentration on the remelted area attests that superficial layer was enriched with oxygen during laser processing, which is beneficial for increasing the resistance to high temperatures in corrosive-erosive metallic environments.

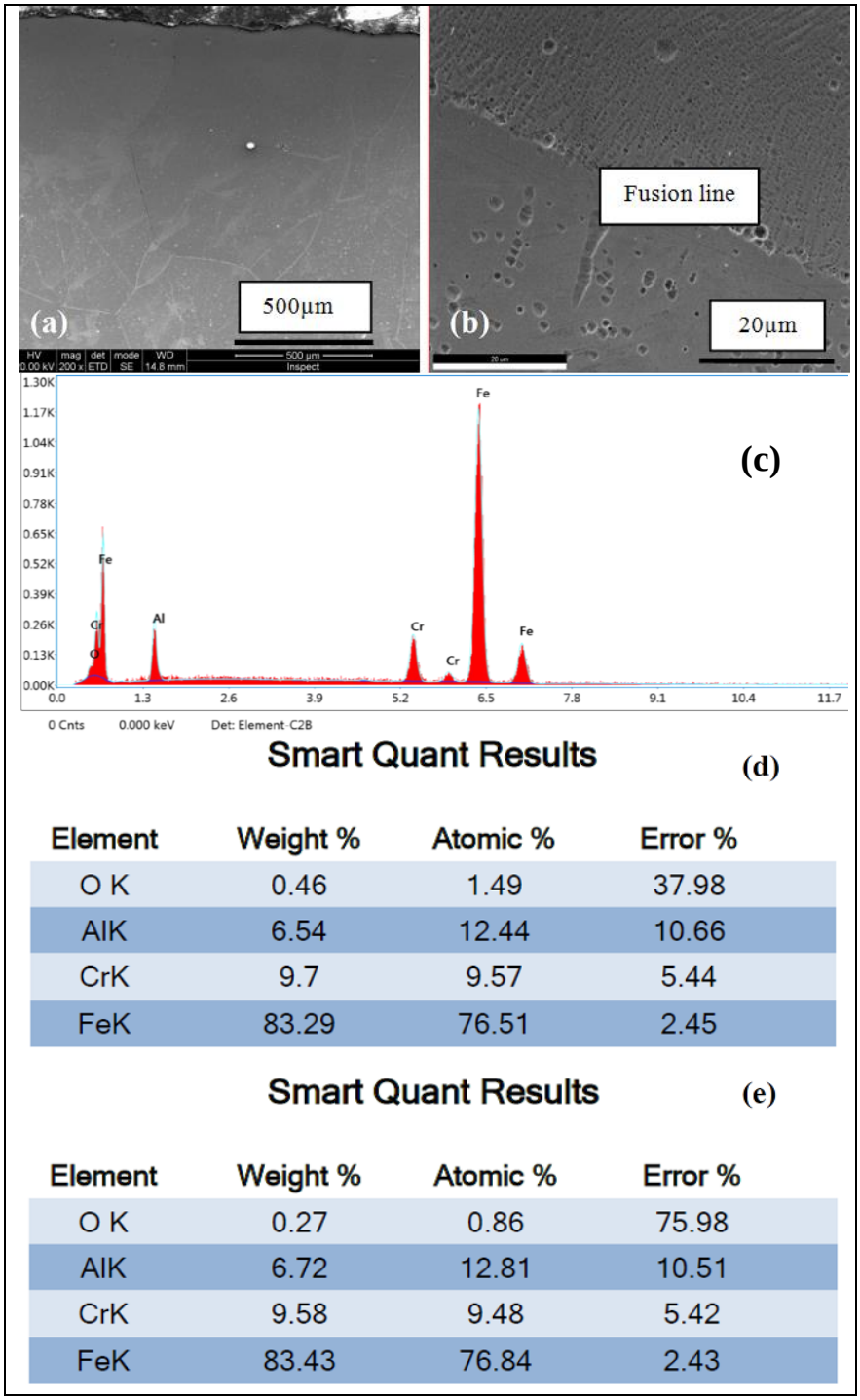

Smart Quant Results (d)

Element	Weight %	Atomic %	Error %
O K	0.46	1.49	37.98
AlK	6.54	12.44	10.66
CrK	9.7	9.57	5.44
FeK	83.29	76.51	2.45

Smart Quant Results (e)

Element	Weight %	Atomic %	Error %
O K	0.27	0.86	75.98
AlK	6.72	12.81	10.51
CrK	9.58	9.48	5.42
FeK	83.43	76.84	2.43

Fig. 4. Cross sections of laser processed area analysis of Sample 1: a) the processed area with regime 1; b) detail on the interface between the remelted area and the unprocessed base material (Fusion line); c) EDS spectrum of the elements identified in the laser processed area; d), e) chemical compositions on micro-zones determined by EDAX analysis for the laser remelted area (d) respectively for the base material (e) (color online)

In the case of using a laser power of 500W, the evolution of chemical concentration remains in the same domain, with a slow decrease of Cr (9.35 wt.%) and Al (6.52 wt.%). For Sample 2 (Fig. 5) has been observed a similar microstructure and evolution of the chemical composition. In the laser remelted layer the concentration of chromium and aluminium was: Cr (10.93 wt.% to 11.01 wt.%); Al (5.68 wt.% to 5.78wt.%), close to the concentration measured in transition zone through base material, i.e. Cr (10.95 wt.% to 11.11wt.%) and Al (5.7 wt.% to 5.72 wt.%). The oxygen concentration in the laser remelted layer was of 0.39 wt.% O. All these chemical concentrations are comparable with those of the base material (Table 1).

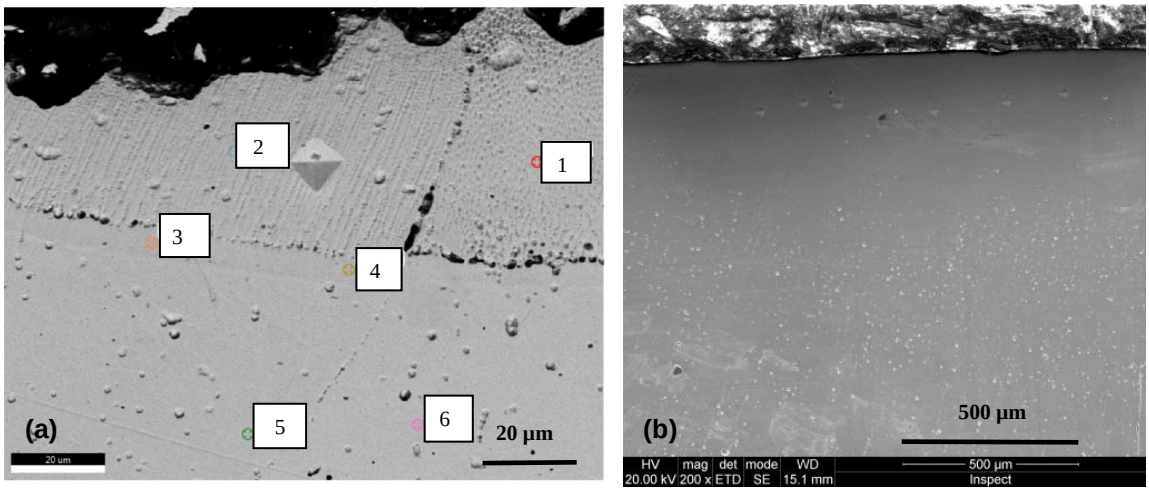

Fig. 5. Cross sections of the laser processed layers of Sample 2: a) regime 1; b) regime 2

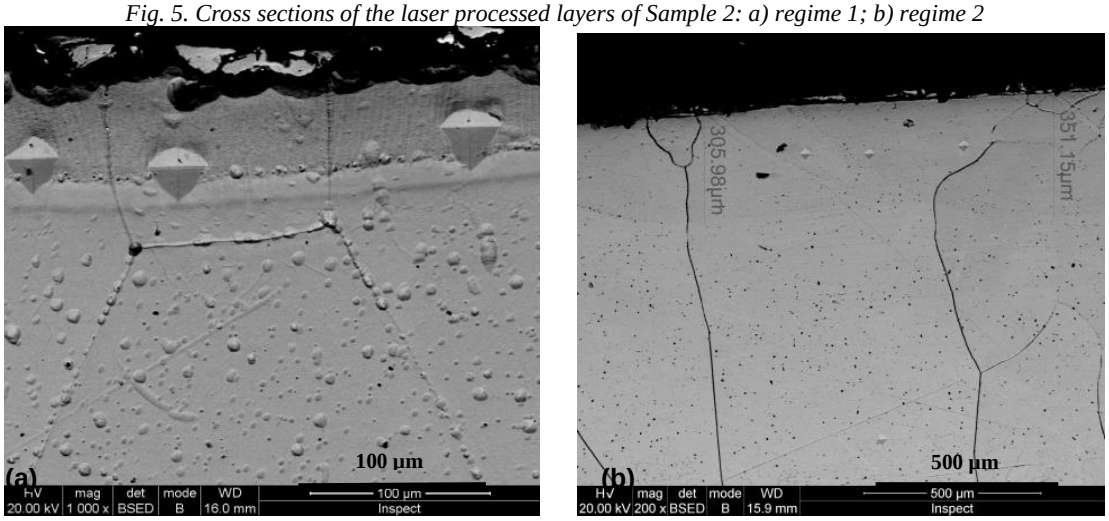

Fig. 6. Cross sections of laser processed layers of Sample 3: a) regime 1; b) regime 2

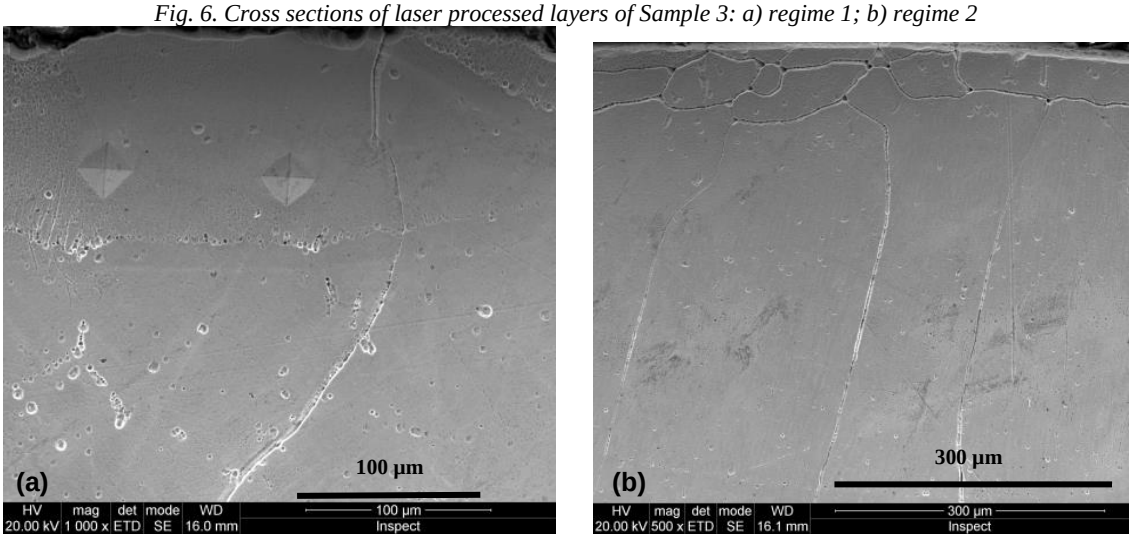

Fig. 7. Cross sections of laser processed layers of Sample 4: a) regime 1; b) regime 2

For both Sample 2 and 3 (S2 and S3) (Fig. 6), the difference of the smoothness of cross section profile is clearly visible at different values of processing laser power. This difference results from the superficial tension of the melted metal, influenced by the temperature and cooling rate. For a higher temperature and a longer maintaining time, has been obtained a smoother surface.

In the case of Sample 3, the concentration of main chemical elements was: Cr (15.86 wt.% - 16.17 wt.%); Al (4.67 wt.% - 4.75 wt.%). The oxygen concentration in laser remelted layer was of 0.61 wt.% O.

As undesired effect, in case of both sample 2 and 3 have been observed pores, located at grain-boundary or in remelted area.

The microstructure of Sample 4 revealed a recrystallization effect (small grains formation) in the laser remelted zone (Fig. 7 and Fig. 8). This effect was also observed for Sample 3, but only in a small area (Fig. 3, Sample 3, regime 2).

The surface profile was smooth, both for regime 1 and regime 2. In this case, the concentration of main chemical elements was: Cr (17.71 wt% for regime 1 and 18.28 to 18.55 wt.% for regime 2); Al (4.12 wt.% for regime 1 and 3.85-4.15wt.% for regime 2). The oxygen concentration in laser remelted layer was of 0.64 wt.% O.

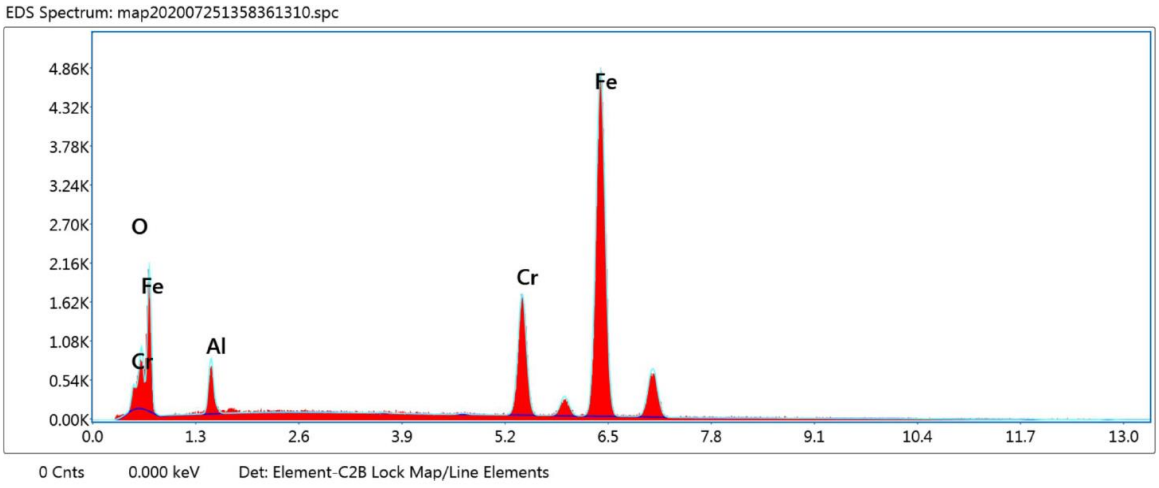

Fig. 8. EDS spectrum of the elements identified in the laser processed area of Sample 4 (color online)

3.2. Microhardness

The microhardness measurements were performed both on base material and laser processed layers, using a Shimadzu HMV 2T microhardness tester. For each zone, 5 different measurements have been performed, using 98mN pressing force and 15 seconds indentation time (Table 3).

Table 3. Average values of HV0.1 microhardness measured on laser processed areas of FeCrAl alloys

Sample	*Regime 1*	*Regime 2*	*Base material*
S1	*265*	*245*	*228*
S2	*255*	*249*	*213*
S3	*238*	*221*	*223*
S4	*242*	*240*	*231*

4. Conclusions

Laser surface processing/remelting led to the formation of a uniform and compact layer, were the intermetallic precipitates from the base matrix have been dissolved. By analysing the layer thicknesses, it results that for regime 1 (laser power of 320W) the penetration depth was between minimum 68 µm (Sample 3) and maximum 163µm (Sample 1). In case of using the regime 2 (laser power of 500W), the penetration depth was between 393 µm (Sample 3) to 519 µm (Sample 1).

For all alloys, it was determined that by laser surface processing can be obtained a fine, dendritic microstructure, with recrystallisation of small grains or preservation of hereditary grains limits and dissolution of the micro-precipitates.

No imperfections such as cracks or layer detachments were identified, but small pores located on the grain boundary have been observed in samples 3 and 4 (having the higher Cr content). There are no internal or external oxidation effects, which prove that the protective atmosphere was appropriate.

The microhardness was higher in the case of regime 1, due to the fast cooling, especially in the case of samples with higher aluminium content (Sample 1).

Acknowledgements

The research work was financially supported by the Romanian National Program for Research in the framework of the Project No. PCCA 243/2014 Advanced

Metallic Materials used for the New Generation of Nuclear Power Plant, 4R – NUCLEARMAT.

References

[1] D. Naumenko, J. Le-Coze, E. Wessel, W. Fischer, W. J. Quadakkers, Mater. Trans. **43**(2), 168 (2002).
[2] V. Geantă, I. Voiculescu, R. Ștefănoiu, A. Jianu, Metal. Int. **XVI**(5), 153 (2011).
[3] H. Al-Badairy, D. J. Prior, G. J. Tatlock, J. Le-Coze, A. R. Jones, Mater. et Tech. **94**, 253 (2006).
[4] J. Checmanowski, A. Matraszek, I. Szczygiel, B. Szczygiel, J. Therm Anal. Calorim **113**, 311 (2013).
[5] M. F. Pillis, L. V. Ramanathan, Mater. Res. **7**(1), 97 (2004).
[6] B. Pint, A. Garrat-Reed, L. Hobbs, J. Phys. **IV**(3)(C9), 247 (1993).
[7] W. J. Quadakkers, J. Phys. **IV** (3)(C9), 177 (1993).
[8] K. Reszka, J. Morgiel, Z. Zurek, A. Jaron, Arch. Metall. Mater. **59**, 77 (2014).
[9] M. Selagea, E. Moraru, D. Besnea, R. Udrea, B. Lungu, Optoelectron. Adv. Mat. **13**(9-10), 539 (2019).
[10] Y. Yamamoto, Y. Yang, K. G. Field, K. Terrani, B. A. Pint, L.L Snead, Letter Report Documenting Progress of Second-Generation ATF FeCrAl Alloy Fabrication, Oak Ridge National Laboratory ORNL/LTR., 1(2014).
[11] S. Bragg-Sitton, Nuclear News **57**(3), 83 (2014).
[12] M. Serrano de Caro, A. K. Woloshun, V. F. Rubio, A. S. Maloy, Materials Selection for Lead-Bismuth Corrosion and Erosion Tests in DELTA Loop, Los Alamos laboratory Report LA-UR-13-22282, 1, (2013).
[13] G. Mueller, W. An, Th. Berghofer, M. Del Giaco, Ch. Eing, R. Fetzer, B. Flickinger, W. Frey et al., J. Korean Phys. Soc. **59**(6), 3588 (2011).
[14] M. Del Giacco, A. Weisenburger, P. Spieler, F. Zimmermann, F. Lang, A. Jianu, G. Mueller, Wear **280-281**, 46 (2012).
[15] T. R. Allen, D. C. Crawford, Sci. Technol. Nucl. Ins. **2007**(3), 1 (2007).
[16] J. Ejenstam, Corrosion resistant alumina-forming alloys for lead-cooled fast reactors, Doctoral Thesis in Chemistry, Stockholm, Sweden, 2015.
[17] M. A. Montealegre, G. Castro, P. Rey, J. L. Arias, P. Vazquez, M. Gonzalez, Contemp. Mater. **I-1**, 19 (2010).
[18] E. Yasa, J. Kruth, Adv. Prod. Eng. Manag. **6**(4), 259 (2011).
[19] Y. Wu, G. Zhang, B. Zhang, Z. Feng, Y. Liang, F. Liu, J. Mater. Sci. Technol. **17**(5), 525 (2001).
[20] A. Temmler, E. Willenborg, K. Wissenbach, Phys. Procedia **12**, 419 (2011).
[21] C. Jinsong, Y. Jianming, Q. Bin, Mater. Trans. **53**(12), 2205 (2012).
[22] I. Avarvarei, O. Dontu, D. Besnea, I. Voiculescu, R. Ciobanu, Optoelectron. Adv. Mat. **4**(11), 1894 (2010).
[23] J. L Ocaña, C. Molpeceres, M. Morales, A. Garcia-Beltran, High-Power Laser Ablation II SPIE Proceedings **3885**, 252 (2000).
[24] A. Rico, F. Sevillano, C. J. Múnez, M. D. López, V. Utrilla, J. Rodríguez, P. Poza, J. Nanosci Nanotechnol. **12**(6), 4984 (2012).
[25] E. M. Stanciu, A. Pascu, M. H. Țierean, I. Voiculescu, I. C. Roată, C. Croitoru, I. Hulka, Mater. Manuf. Process. **31**(12), 1556 (2016).
[26] A. Pascu, E. M. Stanciu, I. Voiculescu, M. H. Țierean, I. C. Roată, J. L. Ocaña, Mater. Manuf. Process. **31**(03), 311 (2016).
[27] V. Geantă, I.Voiculescu, R. Ștefănoiu, D. Savastru, I. Csaki, D. Patroi, L. Leonat, Optoelectron. Adv. Mat. **7**, 874 (2013).
[28] V. Geantă, I. Voiculescu, R. Ștefănoiu, A. Jianu, Metal. Int. **16**(5), 153 (2011).
[29] V. Geantă, I. Voiculescu, R. Ștefănoiu, A. Jianu, I. Milosan, E. M. Stanciu, A. Pascu, I. M. Vasile, Rev. Chim.(Bucharest) **70**(2), 549 (2019).
[30] I. Voiculescu, V. Geanta, E. M Stanciu, D. A Jianu, C. Postolache, V. Fugaru, Acta Phys. Pol. A. **134**(1), 116 (2018).
[31] I. Milosan, M. Florescu, D. Cristea, I. Voiculescu, M. A. Pop, I. Cañadas, J. Rodriguez, C. A. Bogatu, T. Bedo, Materials **13**(3), 1 (2020).
[32] I. Milosan, D. Cristea, I. Voiculescu, M. A. Pop, M. Balat-Pichelin, A. M. Predescu, C. A. Bogatu, T. Bedo, A. C. Berbecaru, V. Geanta, C. Gabor, L. A. Isac, F. A. Sarbu, G. Oancea, Int. J. Adv. Manuf. Technol. **101**(9-12), 2955 (2019).
[33] I. Milosan, G. Flamant, I. Voiculescu, V. Geanta, D. Munteanu, T. Bedo, M. A. Pop, A. Semenescu, A. Crisan, D. Cristea, M. Stoicanescu, C. Gabor, F. A. Sarbu, I. Ghiuta, Rev. Chim. (Bucharest) **69**(5), 1050 (2018).
[34] Y. Tian, J. Ju, H. Fu, S. Ma, J. Lin, Y. Lei, ASM International **28**, 6428 (2019).

*Corresponding author: ioneliav@yahoo.co.uk.